Hindawi Publishing Corporation
EURASIP Journal on Wireless Communications and Networking
Volume 2007, Article ID 35946, 14 pages
doi:10.1155/2007/35946

Research Article

A Markovian Model Representation of Individual Mobility Scenarios in Ad Hoc Networks and Its Evaluation

C. A. V. Campos and L. F. M. de Moraes

High-Speed Networks Laboratory, RAVEL COPPE/Federal University of Rio de Janeiro (UFRJ), RJ, Brazil

Received 15 July 2006; Revised 27 January 2007; Accepted 30 January 2007

Recommended by Marco Conti

Adequate representation of mobility is a very important issue in simulation of mobile ad hoc networks. In this context, we consider the characterization of the mobile nodes movement through a Markovian modeling. Our proposed representation allows for smooth movements and the generation of several different mobility profiles. This approach is also shown to be more suitable for use in various ad hoc networks scenarios than other proposed mobility models, such as the random waypoint (RWP) model. An evaluation of the proposed model is provided, under different border rule scenarios. In addition, the performance of AODV, DSR, and DSDV routing protocols is also studied through simulations, utilizing the proposed model, and the results obtained are discussed.

1. INTRODUCTION

Mobile ad hoc networks (MANETs) are wireless networks that do not need an infrastructure to be set up for communication and data distribution. Thus, a sender node can either forward data directly to the destination device when it is close enough, or through intermediate devices when the destination is out of reach in a single hop. In this context, all the wireless mobile nodes (MNs) must have the capacity to forward data acting as routers. However, in these networks, user mobility adds problems that should be addressed, mainly due to the dynamism of the network topology, diminishing communication link lifetime. As a consequence of this dynamic behavior, the performance of proposed solutions (applications and subsystems) from MANETs is directly affected, forcing researchers to take mobility into account when evaluating developed algorithms and protocols for such networks.

In spite of the huge amount of work and research dedicated to ad hoc networks in the last years, several problems and challenges remain open. For example, since MANETs are still in a development stage, it is quite difficult to obtain mobility traces from real scenarios. As a consequence, the use of synthetic mobility models, that try to represent the MNs movement behavior becomes necessary in order to simulate user mobility profiles. Several mobility models have been proposed in the past few years, but they present some problems, such as mean speed decay with time and sudden changes in movement direction and speed.

In the present work, a detailed study of the motion behavior of MNs and its impact on the routing protocol performance for MANETs are presented.

The rest of this paper is outlined as follows. In Section 2, we describe the main published works about mobility models available for MANETs. Our proposed Markovian modeling and the characterization of different mobility profiles allowed by it are presented in Section 3. Section 4 presents an analysis for the impact of border rules on the proposed mobility model. In Section 5, we present the performance evaluation for AODV, DSR, and DSDV routing protocols, which result from simulations using the proposed mobility model. Finally, Section 6 concludes the paper, highlighting the main contributions of our work, and proposing some directions for future research.

2. MOBILITY IN MANETs

As mentioned before, mobility models are used to represent the mobility patterns of an MN. These models are used in performance evaluations of applications and communication systems, allowing analysis of the impact caused by mobility on their functioning. Mobility models can be applied in many studied environments, such as the management of

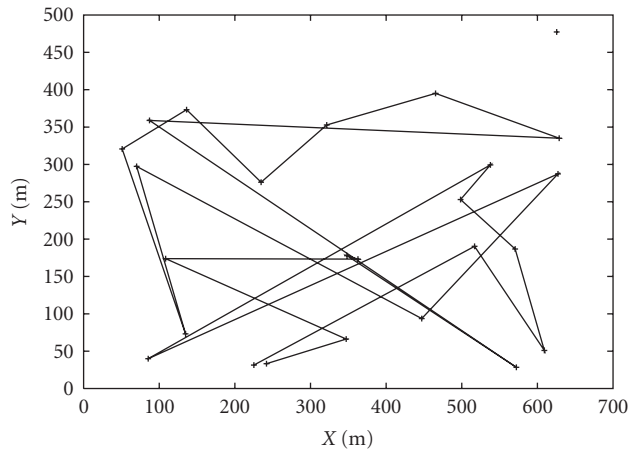

Figure 1: Course taken by one MN using the RWP model.

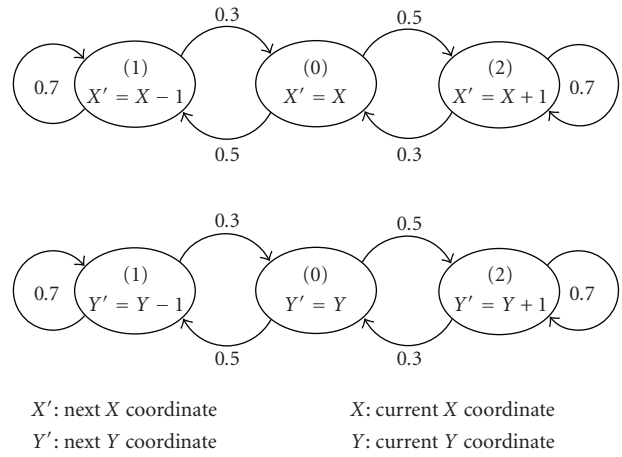

Figure 2: MRP model.

cryptographic key distribution, packet-loss evaluation, traffic management, performance evaluation of routing protocols [1, 2], partition prediction, service discovery in partitionable networks [3], and medium access protocols for MANETs, among others.

These models can be further classified in two categories: Individual mobility models (IMM) and group mobility models (GMM). Thus, these categories and mobility related to previous works are described below.

2.1. Individual mobility models

IMMs represent the movement pattern of an MN independent of other MNs in the neighborhood, and are the most used models in performance evaluation of MANETs [1]. In this section, some IMMs will be briefly described.

One of the most used mobility models in MANET simulation is the *random walk* mobility model [4]. In this model, the movement direction and speed at some time $t + \Delta t$ has no relationship with the direction and speed at time t. This characteristic makes this model memoryless, and generates a nonrealistic movement for each MN, presenting sharp turns, sudden stops, and accelerations. Some other models based on the random walk mobility model have also been proposed [5, 6].

The *random waypoint* (RWP) model, described in [7], divides the course taken by the MN into two periods, the movement period and the pause period. The MN stays at some place for a random amount of time (*pause time*) and then moves to a new place chosen randomly with a speed that follows an exponential distribution between [minspeed, maxspeed], as shown in Figure 1. Nowadays, this is the most widely used model. This model is also memoryless, and has the same drawbacks of the random mobility model. In [8–11], studies about the harmful behavior of RWP model are presented, mainly about the nonstationarity behavior. Thus, this model presents undesirable characteristics and that must be taken in consideration in the MANETs simulations.

The markovian random path (MRP) is a probability model proposed by Chiang in [12], which explores a less sudden movement by the nodes. This probability model is controlled by a three-state Markov chain to represent the *movement behavior* in directions x and y on the plane. One should notice that the states of the MCs (for each direction, x and y) in this case represent the position variation and not the X and Y position themselves. Therefore, as shown by Figure 2, the state-transition diagrams of X-direction and Y-direction will represent the direction changes of the MN. Initially, both X-direction and Y-direction are on state E_0; in the next step, going from E_0 to E_2 represents an increase in the respective coordinate (x, or y), and a transition to E_1 will denote a decrease in the respective coordinate (again, x, or y).

In other words, the Markov chains states (0, 1, and 2) control the movement behavior of MNs, instead of directly representing their positions. The reader should refer to [12] for additional details about this mobility model.

In this model, movements in the horizontal and vertical directions as well as stops are not possible for an interval of time greater than one step. Besides that, once the MN starts to move it is likely to remain in the same direction, because the probability to stay in state (1) or (2) of the Markov chain is greater than the probability to go back to state (0). Another property of this model is that it does not allow sudden changes in the movement direction. This is because there are no step transitions between states (1) and (2), that is, before changing direction the MN first has to stop.

Additional models for individual mobility have been proposed in the literature. The work in [13] introduced a discretized version of a Gauss-Markov process to model the MNs velocity in one dimension (a multidimensional extension is presented in [14]). The latter exploits the predictability of user mobility patterns, therefore being more realistic than random-walk or constant-velocity models. In this sense, the Markovian model presented by us is somehow related to that in [13]. However, we further emphasize that, in spite of being related to the work in [13], the Markov chain

model presented here is different. As in [12], the states of the Markov chain here are used to represent changes in motion. In [1] it is presented a boundless simulation area model. The *city section* model is proposed in [1] and tries to represent the movement of an MN in urban environments. In [15], a *smooth* model, which represents motion smoother than in random walk and waypoint models, is proposed. A more realistic model where obstacles in the scenario are taken into consideration is proposed in [8].

2.2. Group mobility models

Group mobility models are used to represent the movement of a group of MNs. These models have recently been used to predict the partitioning of MANETs, which is defined as a wide-scale topology change, caused mainly by the group movement behavior of the MNs.

A group mobility model developed by Hong et al. in [16] is the group point reference mobility (GPRM) model. For each MN there is an associated reference point which states the group movement. The MNs are initially placed randomly around the reference point within a geographical area. Each reference point has a group movement vector, which is added to the random movement vector of each MN to determine the next position of the respective MN. The GPRM model defines the group movement explicitly, determining a movement path for each group.

2.3. Frameworks for mobility models

Recently, researchers have been seeking to represent mobility, not only through mobility model development, but through synthetic environment representations and user movement analysis in possible MANET scenarios.

In [15], a conceptual map of mobility representation used in the simulation and analysis of wireless systems is presented. This representation is performed through the components: randomness level (deterministic, hybrid, or random), detailing level (micromobility, macromobility, individual, and group movements), simulation or analytical representation, and representation dimensions (1D, 2D, or 3D). Moreover, in the random approach, several border rules are used to choose new movement directions. This representation can be applied in both infrastructureless and infrastructured wireless networks. Such proposal characterizes mobility in an interesting and comprising way; however, evaluation metrics of mobility or conceptual map components are not defined. This limits simulation evaluations that follow this modeling. It is important to notice that this was a first attempt of mobility representation through a framework for MANETs.

Important is a framework proposed in [17], to systematically analyze the mobility impact on the performance of the routing protocols for MANETs. For this, mobility and connectivity graph metrics were proposed, independently of the protocols. The frameworks comprise the following aspects: mobility models, metrics for the mobility and connectivity graph characterization, and the relationship between mobility and the routing performance.

This framework has the following contributions:

(i) focuses on the mobility characteristics, such as spatial dependence, geographical restrictions and temporal dependence;
(ii) definitions of metrics of the connectivity graphs, studying the interaction of mobility metrics with the connectivity metrics and its effects on the protocols' performance;
(iii) analyses of the reasons for the differences in the protocol performance as a whole, through the investigation of the mobility of the parts that compose the protocol effect.

This framework is a great contribution to mobility model evaluation, aiming at the level of realism of the models for the simulation of mobility in MANETs. Therefore, the proposed metrics to evaluate the movement behavior and the network topology are totally independent from the protocols, which allow a mobility model behavior evaluation. The proposed metrics in [17], provided new insights in the performance evaluation of the routing protocols.

3. PROPOSAL OF AN ALTERNATIVE MODELING FOR INDIVIDUAL MOBILITY

As presented in Section 2, user movement representation is important and necessary for a preliminary analysis of the application behavior used in MANETs. This representation allows a detailed and in-depth study of these networks, even without a real world implementation.

As in [18], a Markov chain model is used in this paper. In addition, the proposed modeling can be characterized by Bettstetter's framework [15], where a random approach for the direction and speed change was applied with probabilistic values distributed nonuniformly. Modeling can represent several dimensions; however, as a framework detailing level it can represent only individual movements. In the direction choice, all the border rules of the framework can be used.

The proposed models are based on [12] and Markovian processes [18], and will be detailed in the following subsections.

3.1. Simple individual Markovian mobility model

As described in Section 2, the MRP model tries to describe the movement with a more adequate behavior than the random walk and RWP models. However, in accordance with the description given in Section 2.1, we notice that the MRP model does not allow the following: (i) vertical or horizontal movements; (ii) pause durations of two or more consecutive time intervals (in other words, pauses, whenever they occur, can last at most one time interval); and (iii) smooth changes of speed.

In this way, an extension of the MRP model is proposed supporting such characteristics. This extension is denominated *simple individual markovian mobility (SIMM)* model. In the next sections, analytical modeling and mobility profile generation will be addressed.

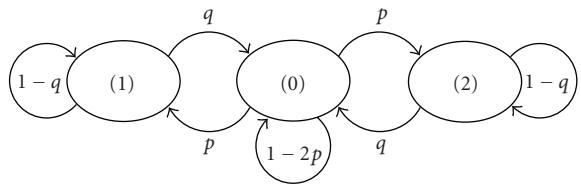

Figure 3: State transition diagram for the Markov chains representing movement in the SIMM model (for both x- and y-directions).

Table 1: Possible motion representation of state $(0,0)$ given by state-transitions of the SIMM model.

Transitions from → to	Motion representation
$(0,0) \longrightarrow (0,0)$	$X' = X; Y' = Y;$
$(0,0) \longrightarrow (2,0)$	$X' = X + D; Y' = Y;$
$(0,0) \longrightarrow (0,2)$	$X' = X; Y' = Y + D;$
$(0,0) \longrightarrow (1,0)$	$X' = X - D; Y' = Y;$
$(0,0) \longrightarrow (0,1)$	$X' = X; Y' = Y - D;$
$(0,0) \longrightarrow (2,2)$	$X' = X + D; Y' = Y + D;$
$(0,0) \longrightarrow (1,1)$	$X' = X - D; Y' = Y - D;$
$(0,0) \longrightarrow (1,2)$	$X' = X - D; Y' = Y + D;$
$(0,0) \longrightarrow (2,1)$	$X' = X + D; Y' = Y - D;$

3.1.1. Analytical modeling

The SIMM model uses two Markov chains with discrete parameters and 3 states (0, 1, and 2), to represent movements in the x- and y-coordinate, with changes in coordinates x and y assumed to be independent. Figure 3 illustrates the state transition diagram for the above-mentioned chains (the same for both x- and y-coordinate). As noted, the transition probabilities from state (0) to the other states are defined by p; on the other end, the transition probabilities from both states (1) and (2), to state (0), are defined as q.

Figure 3 illustrates the SIMM model state transition diagram. As it can be observed, this model presents a new characteristic which is to allow transitions from state (0) to itself, with probability $(1 - 2p)$, thus assuming that MNs can remain in that state for one or more consecutive steps. The model allows every MN to remain still, that is, x and y remain the same in one or more instants of time. However, the permanence in states (1) or (2) is given by the probability $(1 - q)$.

Considering the extensions to MRP mentioned in the previous paragraph, the SIMM model assumes that the discrete-parameter Markov chains representing the shift in directions x and y allow transitions to take place from state (0) to itself. Also, instead of representing the changes in each direction by individual Markov chains, as shown in Figure 2, the SIMM model utilizes a two-dimension state vector (i, j); with $i, j \in \{0, 1, 2\}$. Therefore, the analytical model for SIMM utilizes a vector Markov chain with state space given by $S = \{0, 1, 2\} \times \{0, 1, 2\}$, where each of the components, i and j, are used to describe the shifts in directions x and y, respectively. In addition, with respect to the motion in each direction, the SIMM model generalizes the assumption made by the MRP model by allowing the shift in position (in either direction, x and/or y) to take an absolute value equal to D units (where D is an integer > 1). Thus, the SIMM model is seen to generalize the MRP model. We note that, in the particular case of the SIMM model when $D = 1$, and transitions from the vector state $(0,0)$ to either state $(0, j)$ or $(i, 0)$ with $i, j \in S$, and vice-versa, are not allowed; so, it will represent the same behavior as in the MRP model. Looking at the state transition diagram shown in Figure 4, we emphasize that the states are given by the vector (i, j), with $i, j \in S$.

We define P_{SIMM} as the one-step, stationary transition probabilities matrix associated to the (homogeneous) Markov chain representing the SIMM model,

$$P_{\text{SIMM}} = \begin{bmatrix} A^2 & Ap & Ap & Ap & Ap & p^2 & p^2 & p^2 & p^2 \\ Aq & AB & 0 & pq & pq & Cp & 0 & Cp & 0 \\ Aq & 0 & AB & pq & pq & 0 & Cp & 0 & Cp \\ Aq & pq & pq & AB & 0 & Cp & Cp & 0 & 0 \\ Aq & pq & pq & 0 & AB & 0 & 0 & Cp & Cp \\ q^2 & Bq & 0 & Bq & 0 & B^2 & 0 & 0 & 0 \\ q^2 & 0 & Bq & Bq & 0 & 0 & B^2 & 0 & 0 \\ q^2 & Bq & 0 & 0 & Bq & 0 & 0 & B^2 & 0 \\ q^2 & 0 & Bq & 0 & Bq & 0 & 0 & 0 & B^2 \end{bmatrix}, \tag{1}$$

where $A = (1 - 2p)$, $B = (1 - p)$, and $C = (1 - q)$.

Starting at position X, Y, which in the state diagram is given by $(0,0)$ of the Markov chain, the transitions illustrated represent, respectively, the motion representation given in Table 1.

Given that the MN has been for the state $(2,0)$ the possible transitions are shown with the respective motion representations described in Table 2.

Table 2: Possible motion representation of state $(2,0)$ given by state-transitions of the SIMM model.

Transitions from → to	Motion representation
$(2,0) \longrightarrow (2,0)$	$X' = X + D; Y' = Y;$
$(2,0) \longrightarrow (2,1)$	$X' = X + D; Y' = Y - D;$
$(2,0) \longrightarrow (0,0)$	$X' = X; Y' = Y;$
$(2,0) \longrightarrow (2,2)$	$X' = X + D; Y' = Y + D;$
$(2,0) \longrightarrow (0,2)$	$X' = X; Y' = Y + D;$
$(2,0) \longrightarrow (0,1)$	$X' = X; Y' = Y - D;$

Assuming that the MN is in the state $(2,2)$, Table 3 shows the possible motion representations.

According to this characteristic, the SIMM model can represent movements with just three velocity values $\{0, D, D\sqrt{2}\}$ m/s or Km/h. Thus it is indicated for scenarios of small velocity variations, such as WLAN, bluetooth, and sensor network applications with restricted mobility.

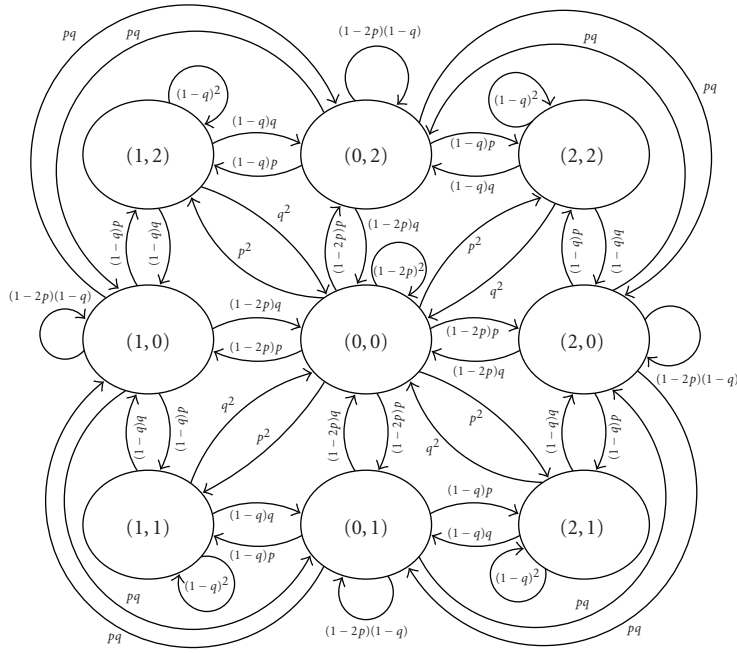

Figure 4: Example of state-transition diagram for the SIMM model—the components i and j (of the two-dimension vector states (i, j)) describe the shifts made by the mobile node (MN) in directions x and y, respectively.

Table 3: Possible motion representation of state $(2,0)$ given by state-transitions of the SIMM model.

Transitions from → to	Motion representation
$(2,2) \longrightarrow (2,2)$	$X' = X + D$; $Y' = Y + D$;
$(2,2) \longrightarrow (0,2)$	$X' = X$; $Y' = Y + D$;
$(2,2) \longrightarrow (0,0)$	$X' = X$; $Y' = Y$;
$(2,2) \longrightarrow (2,0)$	$X' = X + D$; $Y' = Y$;

From P_{SIMM} matrix and in Figure 4 the following characteristics in the SIMM model can be observed.

(1) The probability that an MN remains stopped at a point in time is given by $(1-2p)^2$. If p has a large value, this model will allow very few stops.
(2) The probability that an MN remains moving in the same (vertical and horizontal) direction is given by $(1-2p)(1-q)$ if p has a very few moves in these directions. Besides that, as q increases, fewer will be moved into these directions.
(3) The probability that a MN remains moving in the same (diagonal) direction is given by $(1-q)^2$. This way, the less is the value of q, the greater will be to move into this direction.

As it was described in the characteristics above, varying p and q probabilities values, between [0, 0.5], a behavior variety is generated by SIMM model, characterizing it so, as a reconfigurable and adaptive model to specific situations. To this degree, this model will allow the generation of the several nodes mobility profiles in a network. These profiles will be detailed in the following section.

3.1.2. Mobility profiles

A mobility profile can be defined as being a subgroup of values attributed to each characteristics, correlating them within MN movement following a mobility model in a specific simulation area. Thus, each mobility profile represents a specific movement behavior.

As characteristics of movement of an MN, these are velocity variation, direction change behavior, stop number in movement, pause time, and MN motion dependence interval with other members of network. Varying the value of each characteristic, it is possible to attain a specific mobility profile.

Likewise, the utilization of the transition probability different matrix permits the generation of several mobility profiles. It is only necessary to attribute different values for the p and q parameters, which will allow specific mobility profiles, as some shown below. Furthermore, on the mobility profile generation the D parameter define the size of the increment in the displacement of the MN in the time. This displacement of the MN in the time gives the MN speed. In this context, if the D parameter to be equal to 1 and transition between the states duration time equal to 1 second, it will produce a displacement of 1 m or 1.41 m per second. As described in Section 3.1.1, the D parameter can be changed. In what follows the SIMM model is used to exemplify the description of different mobility profiles.

SIMMa mobility profile

The SIMMa mobility profile is defined by adjustment of p and q parameters as 0.4 and 0.3, respectively. Thus, P_{xy} matrix transforms itself into the P_a matrix, shown below.

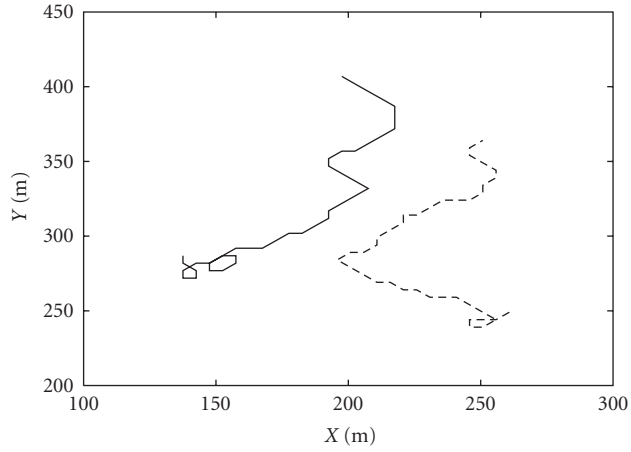

Figure 5: Course of two MNs using the SIMMa profile.

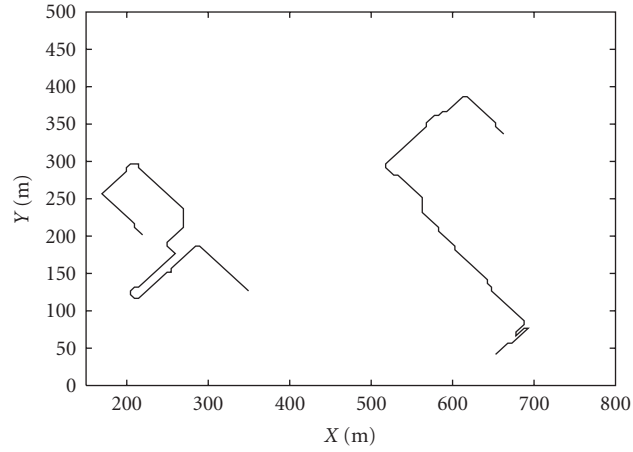

Figure 6: Course of the MN following the SIMMb profile.

From P_a, following characteristics from SIMMa profile can be observed: rare pauses on the movement, small vertical or horizontal movement, and large movement in diagonal directions. This profile can represent the people movement in irregular areas with very rare pauses, as illustrated in Figure 5:

$$P_a = \begin{bmatrix} 0.04 & 0.08 & 0.08 & 0.08 & 0.08 & 0.16 & 0.16 & 0.16 & 0.16 \\ 0.06 & 0.14 & 0 & 0.12 & 0.12 & 0.28 & 0 & 0.28 & 0 \\ 0.06 & 0 & 0.14 & 0.12 & 0.12 & 0 & 0.28 & 0 & 0.28 \\ 0.06 & 0.12 & 0.12 & 0.14 & 0 & 0.28 & 0.28 & 0 & 0 \\ 0.06 & 0.12 & 0.12 & 0 & 0.14 & 0 & 0 & 0.28 & 0.28 \\ 0.09 & 0.21 & 0 & 0.21 & 0 & 0.49 & 0 & 0 & 0 \\ 0.09 & 0 & 0.21 & 0.21 & 0 & 0 & 0.49 & 0 & 0 \\ 0.09 & 0.21 & 0 & 0 & 0.21 & 0 & 0 & 0.49 & 0 \\ 0.09 & 0 & 0.21 & 0 & 0.21 & 0 & 0 & 0 & 0.49 \end{bmatrix}. \quad (2)$$

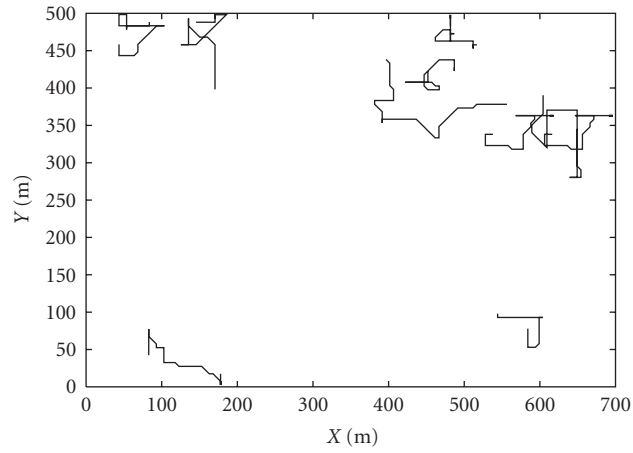

Figure 7: Courses of the various MNs using the SIMMc profile.

SIMMb mobility profile

SIMMb mobility profile is defined by $p = 0.4$ and $q = 0.15$. From these values, the following characteristics from SIMMb profile can be observed in Figure 6: rare pauses in the movement, small movement in the vertical and horizontal directions, and a very large movement in the diagonal directions.

SIMMc mobility profile

SIMMc mobility profile is defined by $p = 0.05$ and $q = 0.2$. From these values, the following SIMMc profile characteristics are made evident: various pauses with a high possibility of remaining still in consecutive time instants, furthermore, there is a frequent motion in all directions. However, as can be seen in Figure 7, the movement is very curvelinious, irregular, and with many pauses, characterizing a small displacement during the simulation time. This profile can represent disaster situations, where MNs have irregular movements and remain still for long periods of time.

SIMMd mobility profile

SIMMd mobility profile is defined by $p = 0.05$ and $q = 0.05$. From these values, the following characteristics can be observed: rare pauses due to transition to state being equal to 0.05; however, with large possibilities of remaining still for a long time. Moreover, there is a high dynamism in all directions, mainly in the diagonals, characterizing rectilinear movements like in some urban regions. This behavior can be seen in Figure 8.

As it was presented in Section 3.1.1, the SIMM model allows vertical and horizontal movements, as well as pauses in the movements during one or more time intervals. In addition, with adjustments of fine parameters, the model generates various mobility scenarios, as described in Section 3.1.2. Nevertheless, the SIMM model does not allow velocity variations in the same direction. Therefore, a generic model will be presented in the next section.

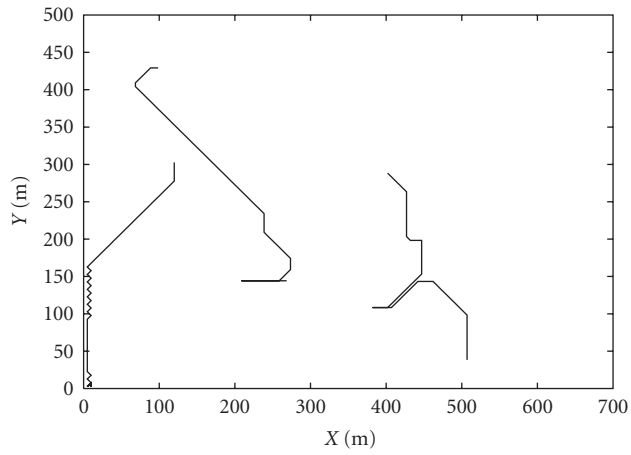

Figure 8: Course of various MNs using the SIMMd profile.

3.2. Generic individual mobility Markovian model

In most scenarios where MANETs are used, MNs move changing their speeds. In order to represent different mobility patterns in a more realistic way, we propose next a generic Markovian model which is able to support a broader range of possibilities concerning speed variations; this is going to be called the generic individual markovian mobility (GIMM) model. In the latter, the absolute value of the position increments can be a real number in the interval $[1, \Delta_{\max}]$. By allowing the increments in position to assume absolute values in this more general interval, a broader range of speeds, corresponding to MNs moves, from a current position, X, to the next position, X', can be represented.

As for the SIMM model (see Section 3.1.1), the GIMM model is also based on two discrete parameter Markov chains to represent the movements in the x and y directions, with changes in coordinates x and y assumed to be independent. However, as a consequence of the broader range of values that can be assumed by changes in MNs position (in each direction), the state space of those chains are now going to be given by $S = \{-e, -e+1, \ldots, -1, 0, 1, \ldots, e-1, e\}$. Here, the states $k \neq 0$ correspond to changes from current position X (or Y) to next position X' (or Y'); and state $k = 0$ represents no change in the corresponding coordinate (i.e., $X = X'$ and/or $Y = Y'$).

Moreover, in the definition above, the state represented by e corresponds to the absolute value of the maximum change in position allowed in a single move of an MN (in each direction, x or y). Therefore, considering the fact that the absolute value of position increments are in the interval $[1, \Delta_{\max}]$, the states (e) and $(-e)$ must correspond to a move from current position X (or Y) to next position $X' = X \pm \Delta_{\max}$ (or $Y' = Y \pm \Delta_{\max}$).

We further emphasize that the states of the Markov chains defined above represent *changes in positions* (for each coordinate, x and y), and not the positions themselves.

For this model, the absolute value of the velocity variation is given by a truncated geometric random variable distributed between 1 and b^{e-1}, where $b > 1$ and $b \in \mathbb{R}$ is the base of the number representing the increments in positions ($X \to X'$, or $Y \to Y'$).

Therefore, by the definitions given above, we have

$$\Delta_{\max} = b^{e-1} \quad \text{for } e > 0. \tag{3}$$

Thus, the correspondence of the states in the Markov chains (for directions x and y) with the changes in positions (see Figure 9) allow the next position of an MN to be obtained as follows:

$$\begin{aligned} X' &= X + s \cdot b^{\alpha} \quad \text{for } 0 \leq \alpha \leq e-1; \\ Y' &= Y + s \cdot b^{\alpha} \quad \text{for } 0 \leq \alpha \leq e-1. \end{aligned} \tag{4}$$

In the above, $s \in \{-1, 0, 1\}$ is used to represent the motion direction (-1 for opposite way, 0 for unchanged position, and 1 for the same way) and the parameter α is an integer number in the interval $[0, e-1]$.

In order to compute the transition probabilities for the state transition diagram in Figure 9, we are going to define $p_{k,j}$ as being the probability of going to state (j) on the next interval, given that we are currently at state (k).

In what following, we summarize the steps to get transitions probabilities for the Markov chain in Figure 9.

Looking to each state of the chain in Figure 9, except for states (e) and $(-e)$, we have the following.

(i) m is the sum value of all transition probabilities to any state at the right-hand side of the current state, given the rules of the state transition diagram for the Markov chain in this Figure. This sum is given by a finite geometric series with ratio 1/2. This value is defined in (5) for state (0) and also for positive states; and in (6) for negative states.

(ii) The sum of all transition probabilities to any state at the left-hand side of the current state is also equal to m, given the rules of the state transition diagram as shown in Figure 9. This value is defined in (7) for state (0) and also for negative states; and in (8) for positive states.

(iii) To stay at current state the value is equal to $(1 - 2m)$, as defined in (9):

$$\sum_{j=k+1}^{e} p_{k,j} = m \quad \text{for } 0 \leq k < e, \tag{5}$$

$$\sum_{j=k+1}^{0} p_{k,j} = m \quad \text{for } -e \leq k < 0, \tag{6}$$

$$\sum_{j=k-1}^{-e} p_{k,j} = m \quad \text{for } -e < k \leq 0, \tag{7}$$

$$\sum_{j=k-1}^{0} p_{k,j} = m \quad \text{for } 0 < k \leq e, \tag{8}$$

$$p_{k,k} = 1 - 2m \quad \text{for } -e < k < e. \tag{9}$$

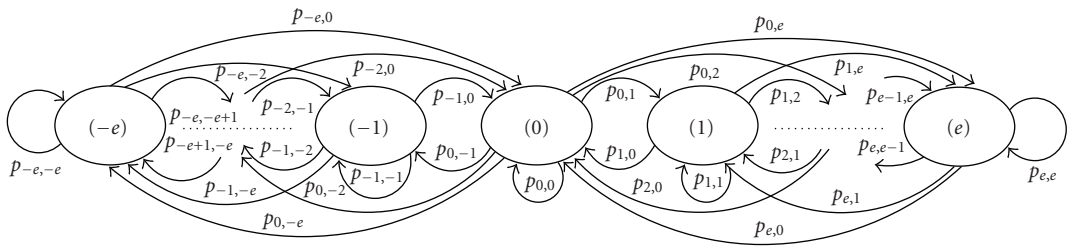

Figure 9: State transition diagram for the Markov chains representing movement in the GIMM model (for both x- and y-directions).

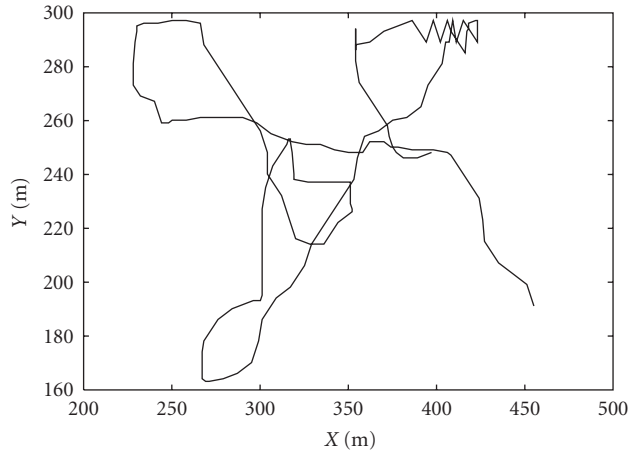

Figure 10: Course of MN using GIMMa profile.

Unlike the other states, $(-e)$ and (e) are the Markov chain edges as shown in Figure 9. The state $(-e)$ only has transition to other states at its right-hand side until the state (0), in which the sum of all possible probability values is equal to m, as defined in (6), or to itself, with the probability value of $1-m$, as defined in (10). In a symmetrical way, state (e), only has possible transition to other states at its left-hand side, in which the sum of all possible probability values until the state (0) is also equal to m, as defined in (7), or to itself, with the probability value of $1-m$, as defined:

$$p_{e,e} = p_{-e,-e} = 1 - m. \tag{10}$$

In addition, from the model assumptions and (5)–(8), we note the following:

$$\begin{aligned} p_{k,j} &= \frac{m2^{(k-j)}}{1-2^{(k-e)}}, \quad \text{with } (0 \le k < e,\ k < j \le e) \\ &\qquad \text{or } (-e < k \le 0,\ -e \le j < k); \\ p_{k,j} &= \frac{m2^{(k-j)}}{1-2^{(-k)}}, \quad \text{with } (-e \le k < 0,\ k < j \le 0) \\ &\qquad \text{or } (0 < k \le e,\ 0 \le j < k). \end{aligned} \tag{11}$$

(i) Velocity increases exponentially until $\Delta_{\max}$ value.

(ii) Once in state ($k \to$ *positive*), it is not possible to change to a state ($k \to$ *negative*) without passing through state (0) and vice versa. With this, the GIMM model avoids sharp turns.

Moreover, the GIMM model can still represent patterns that only increment the position by one (like the SIMM model), and also increment the position by arbitrary values within $[1, \Delta_{\max}]$ (for the coordinates x and y). This way, the GIMM model is generic, allowing the representation of many movement patterns.

3.2.1. Mobility profiles

As defined in Section 3.1.2, mobility profile is characterized by a sub-group which has values attributed by the model parameters. This way, each GIMM model profile represents a specific movement behavior.

To generate different mobility profiles, it is necessary to attribute different values to m, n, and b values, as shown below.

GIMMa mobility profile

The GIMMa profile is defined by the m, e, and b parameter adjustment in the following way: 0.4; 4, and 2, respectively. Therefore, Figure 10 illustrates the behavior of an MN following the GIMMa profile. As the e parameter is equal to 4, this profile reaches its maximum speed of approximately 40 km/h, allowing to represent the displacement of vehicles in a city.

Several other mobility profiles can be represented using the GIMM model, but because of lack of space, only GIMMa was described.

As presented, the GIMM model has the capacity of representing not only patterns with only one increment in the x and y coordinates (e.g., the SIMM model), but also with several increment values in these coordinates, with a smooth variation in this increment. This smoothness is given by the careful adjustment of the transition probabilities between chain states. In other words, it could be said that modeling allows a careful velocity variation, which is an adequate characteristic to represent user . Furthermore, the GIMM model is generic, allowing various pattern representation in user .

An evaluation of presented modeling was described in [19], showing that not only the SIMM model, but also the GIMM model is more adequate and possesses a behavior that is closer to reality than the RWP model. Thus, as proposed models are reconfigurable, these possess a very large applicability potential, needing only to make a fine adjustment of

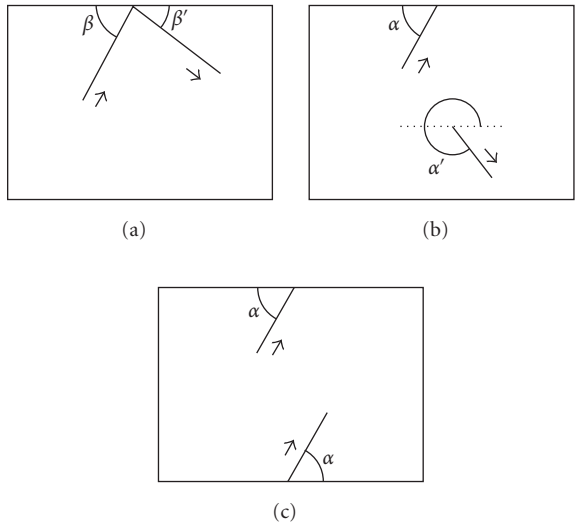

Figure 11: Types of border rules.

their parameters in accordance with characteristics of each profile to be represented.

4. BORDER RULES APPLIED TO THE PROPOSED MODELING

In the literature, there are several border rules [15]. The main rules will be described below: bounce, delete and replace, and wrap around.

4.1. Bounce

The bounce border rule, presented in [15, 20], is defined as being a reflection of the MN movement on the simulation area border, obliging the new course of the MN to remain within the simulation area. This new movement is characterized by two components, β direction angle and s speed, as seen in Figure 11(a). The new value for β' angle will be $-\beta$ in the borders and value of s will remain the same.

There are some extensions of this rule, as presented in [15, 20], in which the new β value is distributed uniformly between $[0, 180°]$, in the superior, inferior, and lateral borders and $[0, 90°]$ in the simulation area corners. The value of s also follows a uniform distribution between [s min, s max].

4.2. Delete and replace

This rule to represent a scenario where the MNs can cross the area border, as it can be seen in many real situations (vehicle movement in highway, entrances, and exits of people in a room). It is defined by this rule that when an MN reaches the border, it is removed from the simulation area and inserted again, randomly inside the simulated area, with a new direction angle α', which can be seen in Figure 11(b).

This rule has the characteristic of representing the exit of the MN from the simulation area, which sometimes is a realistic characteristic. This rule, however, has an undesirable characteristic that is placing of same MN randomly in any position in the area, to avoid that the scenario remains without MNs during the simulation.

4.3. Wrap around

This rule uses the reflection mechanism from the MN movement in the opposite border the frontier. This movement reflection preserves the same α angle and s speed from the MN in the movement reaching the border, as illustrated in Figure 11(c).

With the aim of evaluating the impact from border rules on the GIMM model, Figure 12 shows sharp turn the number of each node with the direction change angle $\geqslant 90°$. For this, the same simulation environment configuration described in [19] and sharp direction turn metric defined as being sharp when the movement direction change angle is in the interval $[90°, 180°]$. This metric indicates if the turns in direction are smooth or not, because a user usually changes direction with an angle of $90°$ maximum. So, a change in an angle bigger than $90°$ is considered sharp. This evaluation was not made in the RWP because the border rule insertion would modify its basic functioning.

Figure 12(a) illustrates this number when it uses the bounce rules and in Figure 12(b) the impact to modified bounce rule. As the second rule is a variation of the first one, they have similar behaviors, which explain the similar impact on the sharp turn change metric. Contrasting this, in Figures 12(c) and 12(d), the GIMM model used the wrap around and delete replace rules, respectively, in which it is possible to observe a small decrease in the sharp change number when compared with the previous rules. Thus, it is possible to conclude that there is a variation in the direction change behavior when a different border rule is used.

Within this context, there should be criteria for the choice of border rule and should be used carefully, for these rules influence the performance evaluation of both systems and simulated applications.

5. IMPACT OF THE MOBILITY MODELS ON THE PERFORMANCE OF THE MANETs

The impact of the mobility models on the routing protocols will be evaluated in this section. This evaluation has the aim of showing the importance of the mobility model and border rule criteria choice to represent a specific environment, as shown in [1, 19, 21]. In contrast, the large majority of the evaluations made in MANETs used the RWP model. To accomplish the routing, it is necessary to utilize the routing protocols. In this manner, the AODV, DSDV, and DSR protocols, which are the most used in MANETs, will be evaluated. The simulation environment and obtained results will be described below.

5.1. Performance metrics

To evaluate the routing protocol performance, it is necessary to use evaluation metrics. In this paper, the following

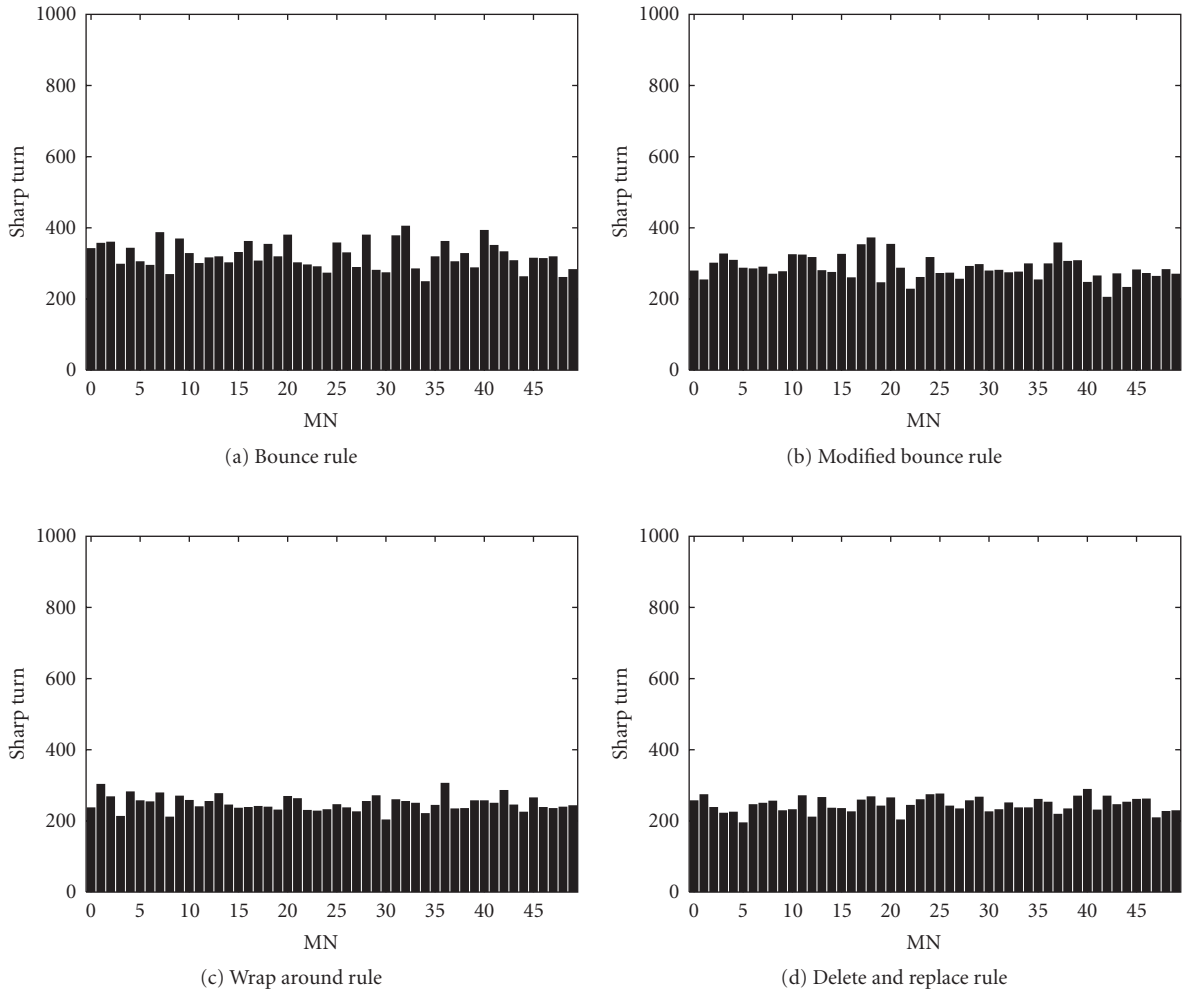

Figure 12: Number of sharp turns with the direction angle change $\geqslant 90^{\circ}$ in the GIMM model with several border rules.

evaluation metrics were used: delivery rate, received packets number, sent packets number, routing packets number, and routing overhead.

(1) *Delivery rate* is defined as being the ratio between the number of the packets received and the number of the sent packets. This metric is used to evaluate the protocol efficiency.
(2) *Number of received packets* is the quantity of the application packets that reached their destiny correctly. This measure is used in the delivery rate metric.
(3) *Number of sent packets* is the quantity of the application packets that are sent by the origin. This measure is also used in the delivery rate metric.
(4) *Number of routing packets* is the discovery and maintenance routes packets quantity sent by the origin or forwarded by the intermediate nodes. This value is necessary for the calculus of the routing overhead in the network.
(5) *Routing overhead* is calculated through the ratio between the quantity of routing packets transmitted in the network and the number of data packets sent by the application. This metric is important to determine the scalability capacity of the protocol, that is, the smaller the banwidth of the network, the smaller should be the routing traffic if compared with the application data traffic. In a congested network, the routing overhead leads to the packet discard, harming the throughput and the discovery and the updating of the routes. Furthermore, the overhead affects the battery energy consumption and with a greater number of routing packets moving through the network, the greater will be the probability of collision. This fact influences not only the delivery rates, but also the end-to-end delay. In the next section, the simulation environment and the obtained results will be described.

5.2. Simulation environment

The network simulator (NS-2 version 2.1b9) [22] was chosen to simulate the MANETs and the ScenGen simulator [23] to

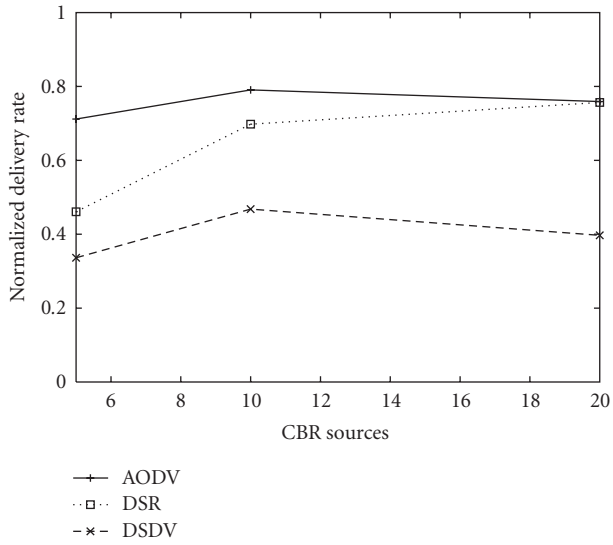

Figure 13: Delivery rate of protocols using the GIMM model.

simulate the mobility models. For the simulation scenarios, a rectangular area of 700 m × 500 m, containing 50 MNs initially positioned in a random way has been used. The mobility models, RWP (min-speed = 0 m/s, max-speed = 12 m/s, pause time = 0 s), SIMM ($p = 0.3$, $q = 0.4$, $D = 5$), and GIMM ($m = 0.4$, $b = 2$, $e = 4$) were used. All the models had average speed approximately equal to 6 m/s. For the GIMM model, the border rules were utilized: bounce, modified bounce, wrap around, delete, and replace were utilized.

As a traffic network specifier, a constant bit rate (CBR) traffic was chosen, instead of the transmission control protocol (TCP) traffic because its congestion control mechanism would affect the protocol evaluation. With the aim of evaluating several charges in the network, 5, 10, and 20 pairs of CBR traffic sources were used in 4 packets of 512 bytes per second rate. These sources were randomly initialized and kept until the end of the simulation. Each evaluated scenario was simulated ten times and the medium value with a confiance level of 0.90 was calculated.

5.3. Achieved results

Figure 13 is presented to verify the traffic influence in the delivery rate of the routing protocols. This analysis was presented only for the GIMM model because of the lack of space. The AODV obtained the highest delivery rate even when the network traffic was increased. In this way, the DSDV, which is a proactive protocol, obtained the worst performance, as it can be verified in most of the performance evaluations available in the literature. For this reason, the DSDV protocol was not evaluated in this paper.

In Table 4, the AODV protocol performance is presented, under the influence of the RWP, SIMM, and GIMM models. In this scenario, the traffic of 10 CBR sources randomly initialized was generated and maintained until the end of simulation (up to 1000 seconds). An enormous variation in the delivery rate with the AODV was observed when the mobility model was switched. Using the RWP, a delivery rate of approximately 94.5% was obtained. However, when the SIMM and GIMM models are used, which were verified to be more realistic than the RWP, this rate decreases to 72.4% and 78.75%, respectively. Thus, this metric decreased approximately 22% between the RWP and the SIMM and of 16% from the RWP to the GIMM.

Table 4: The influence of mobility in the AODV protocol.

Metrics	RWP	SIMM	GIMM
Received packets no.	2334	1799	1753
Sent packets no.	2471	2485	2226
Delivery rate no.	94.46%	72.39%	78.75%
Routing packets no.	8139	34 464	25 337
Routing overhead no.	3.29	13.87	11.38

Table 5: The influence of mobility in the DSR protocol.

Metrics	RWP	SIMM	GIMM
Received packets no.	2333	1948	2020
Sent packets no.	2491	2475	2229
Delivery tax no.	93.66%	78.71%	90.62%
Routing packets no.	3009	76 223	16 954
Routing overhead no.	1.21	30.79	7.61

This decrease on the delivery rate demonstrates that the performance evaluations in the AODV protocol with the RWP model can present an over-estimated value, which can affect the validation of the applications and the subsystem evaluation that use the AODV. The high delivery rate is justified by the fact that the RWP generates around 75% of the sharp turn changes. This means that the MNs remain on average, better distributed within the simulation area which does not happen with the SIMM and GIMM models. In the routing overhead metric, this same behavior is observed, being even more accentuated, seeing as the metric value, using the RWP model, which is approximately 3.3 routing packets propagate for each data packet that is sent. As to the SIMM model, this value increases around 420% in comparison with the RWP value and approximately 340% if compared to the GIMM model. Once more, an over-estimated evaluation of the AODV protocol is identified when the RWP model is used.

In Table 5, the DSR protocol performance is presented using the same mobility models. Again, a large variation is observed in the packet delivery rate under the different mobility models. Using the RWP model, a delivery rate of approximately 93.7% is obtained. However, when the SIMM and GIMM are used, this rate decreases to 78.7% and 90.6%, respectively. Therefore, the delivery rates using DSR under SIMM and GIMM are, respectively, 15% and 3% less than that obtained under the RWP model. The configurations assumed for this scenario are identical to the previous ones.

For the routing overhead metric we observe that approximately 1.2 routing packets propagate for each data packet

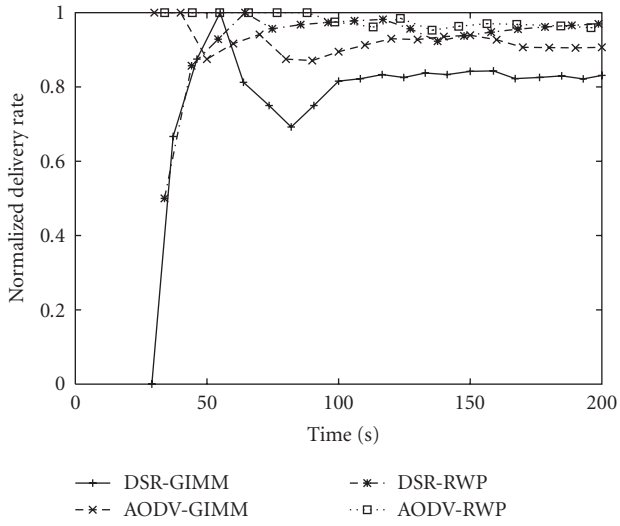

Figure 14: Delivery rate of the AODV and the DSR under the impact of mobility.

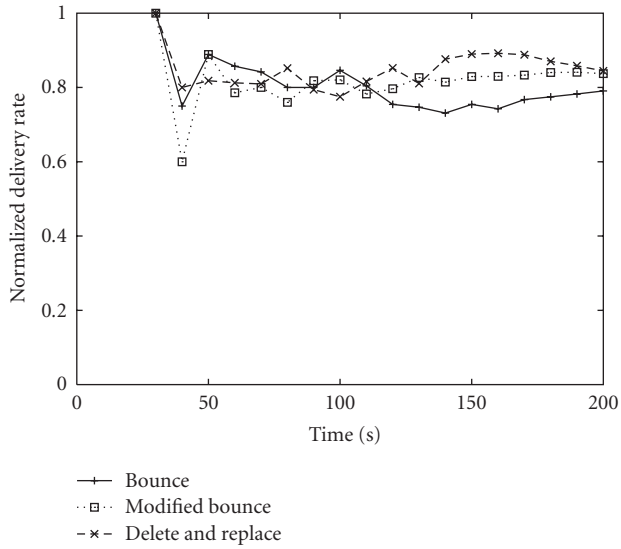

Figure 15: The impact of the chosen border rule on AODV performance.

sent under the RWP model. This value grows around 2400% for the SIMM, and 530% for the GIMM, respectively, as compared to the RWP model. This substantial increase is due to the fact that, in the long range, for SIMM and GIMM the mobile nodes tend to get concentrated in specific regions of the simulation area. Therefore, under the DSR protocol, the nodes tend to generate a great amount of overhead routing packets for each data packet sent. On the other end, since under the RWP model the mobile nodes tend to get better distributed in the simulation area, routes should be available most of the time, a fact that implies in much less overhead, due to routing, per transmitted packet. In Figure 14, the AODV and the DSR protocol delivery rate variation behavior are shown, in relation to RWP and GIMM model simulation time. In this figure, a large delivery rate variation at the beginning of the simulations can be observed, which, as time passes, tends to disappear due to the protocol stability.

With the aim of evaluating the influence of the chosen border rules, Figure 15 was displayed. The bounce and modified bounce generate a very similar impact on the delivery rate and this impact is smaller, around 5%, than the delete and replace rule. These results present an influence of the border rule used in the performance of the routing protocols, which means that the evaluation of these protocols must be done carefully.

Figures 16, 17, and 18 show the impact of the amount of traffic on AODV performance using the border rules: bounce, modified bounce, and delete and replace, respectively. In these figures, the influence that a rule generates in the delivery rate of the protocols with diverse traffics can be observed. These variations prove the necessity of criteria in the utilization of the border rules for the mobility representation in MANETs. In addition, border rules are also parameters to be taken into account in protocol performance evaluations.

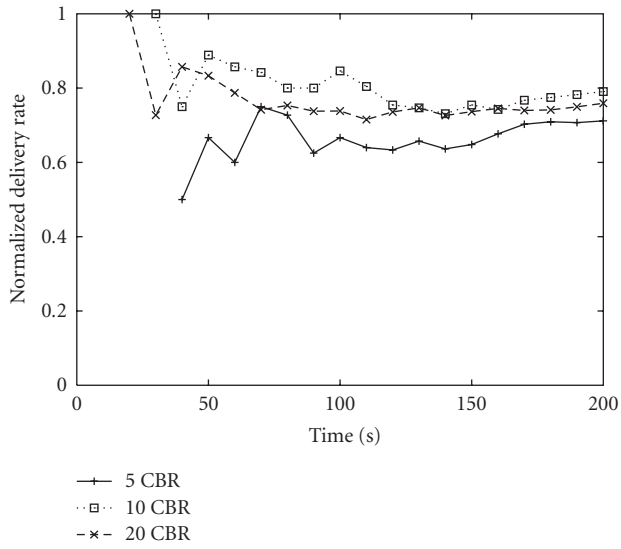

Figure 16: The influence of traffic in AODV performance using the bounce rule.

Finally, new researches on the evaluated protocols are recommended such as, throughput, delay, number of hops, and network density using the above method. Moreover, this evaluation method can also be applied to the evaluation of other routing protocols.

6. CONCLUSIONS AND FUTURE WORK

As described in Section 2, there are several mobility models that are used in MANETs. However, characteristics of these models restrict them to specific behaviors or simply do not

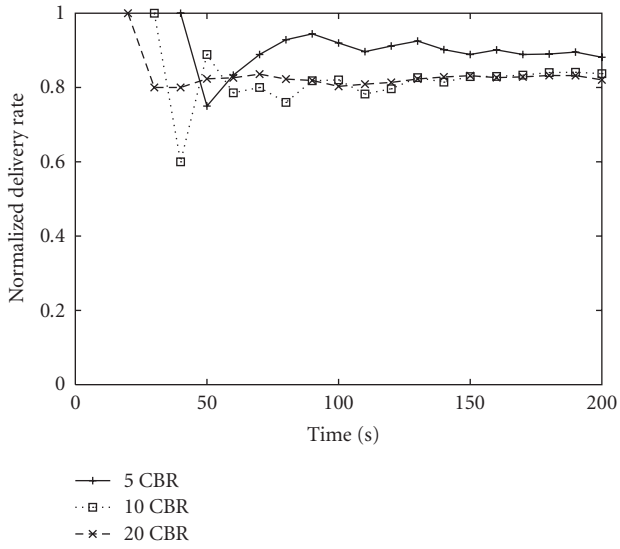

Figure 17: The influence of traffic in AODV performance using the modified bounce rule.

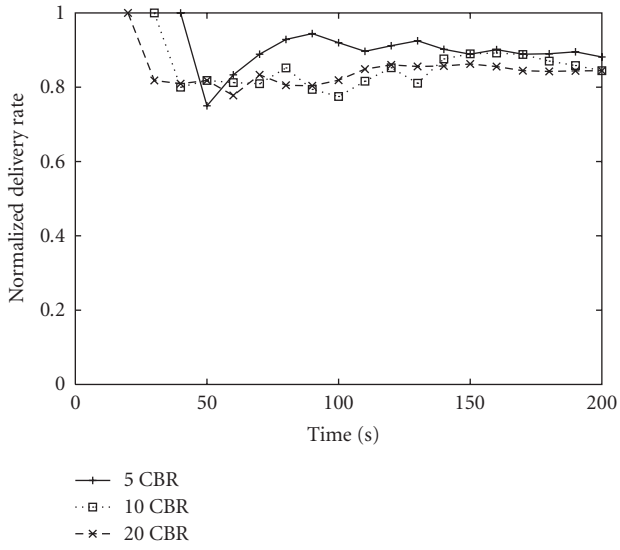

Figure 18: The influence of traffic in AODV performance when applied the delete and replace rule.

represent the reality. Besides, more criteria on the choice of the mobility model are demanded; otherwise, a nonrealistic evaluation as shown in [9, 16, 19, 21] can be made. In this manner, it is necessary to develop new models.

In this context, a mobility modeling was presented, in which the changes of directions and the velocity variations are closer to real scenarios than other existing models in the literature.

The achieved results by simulations verified the modeling characteristics above showing that in certain cases the proposed modeling is more adequate than the RWP model. Moreover, the mobility profiles and border rules were inserted in the modeling, and the impact of these rules was presented.

As an application of the presented modeling, a detailed study of the AODV, DSDV, and DSR routing performance was done. In this evaluation, it was observed that the mobility model and the chosen border rule drastically affect, in some cases, the functioning of these protocols.

The accomplished study showed, utilizing the RWP model, optimistic results; in other words, an over-estimated performance was found. It can be concluded that the chosen mobility model drastically affects the performance evaluation of the routing protocols in MANETs. Thus, this research motivates a reevaluation not only of the routing protocols, but also of all the applications and subsystems of MANETs.

As future works, it is intended to compare the proposed modeling with real data using the methodology proposal in the works of project CRAWDAD [24]. This comparison will be made in relation to the velocity distribution, sharp turn distribution, density of the network, and so forth.

ACKNOWLEDGMENTS

The authors would like to thank Bruno A. A. Nunes and the anonymous reviewers for their criticism and suggestions, which significantly contributed to improve the quality of this paper. This work was sponsored by CAPES (Ministry of Education, Brazil), CNPq, and FINEP (Ministry of Science and Technology, Brazil).

REFERENCES

[1] T. Camp, J. Boleng, and V. Davies, "A survey of mobility models for ad hoc network research," *Wireless Communications and Mobile Computing*, vol. 2, no. 5, pp. 483–502, 2002.

[2] S. R. Das, R. Castaneda, J. Yan, and R. Sengupta, "Comparative performance evaluation of routing protocols for mobile, ad hoc networks," in *Proceedings of the 7th International Conference on Computer Communications and Networks (IC3N '98)*, pp. 153–161, Lafayette, La, USA, October 1998.

[3] K. H. Wang and B. Li, "Efficient and guaranteed service coverage in partitionable mobile ad hoc networks," in *Proceedings of the 21st Annual Joint Conference of the IEEE Computer and Communications Societies (INFOCOM '02)*, vol. 2, pp. 1089–1098, New York, NY, USA, June 2002.

[4] M. M. Zonoozi and P. Dassanayake, "User mobility modeling and characterization of mobility patterns," *IEEE Journal on Selected Areas in Communications*, vol. 15, no. 7, pp. 1239–1252, 1997.

[5] S. Basagni, I. Chlamtac, V. R. Syrotiuk, and B. A. Woodward, "A distance routing effect algorithm for mobility (DREAM)," in *Proceedings of the 4th Annual ACM/IEEE International Conference on Mobile Computing and Networking (MOBICOM '98)*, pp. 76–84, Dallas, Tex, USA, October 1998.

[6] Y. B. Ko and N. H. Vaidya, "Location-aided routing (LAR) in mobile ad hoc networks," in *Proceedings of the 4th Annual ACM/IEEE International Conference on Mobile Computing and Networking (MOBICOM '98)*, pp. 66–75, Dallas, Tex, USA, October 1998.

[7] D. B. Johnson and D. A. Maltz, "Dynamic source routing in ad hoc wireless networks," in *Mobile Computing*, vol. 353,

chapter 5, pp. 153–181, Kluwer Academic, Dordrecht, The Netherlands, 1996.

[8] A. Jardosh, E. M. Belding-Royer, K. C. Almeroth, and S. Suri, "Towards realistic mobility models for mobile ad hoc networks," in *Proceedings of the 9th IEEE Annual International Conference on Mobile Computing and Networking (MOBICOM '03)*, pp. 217–229, San Diego, Calif, USA, September 2003.

[9] J. Yoon, M. Liu, and B. Noble, "Random waypoint considered harmful," in *Proceedings of the 22nd Annual Joint Conference of the IEEE Computer and Communications Societies (INFOCOM '03)*, vol. 2, pp. 1312–1321, San Francisco, Calif, USA, March-April 2003.

[10] W. Navidi and T. Camp, "Stationary distributions for the random waypoint mobility model," *IEEE Transactions on Mobile Computing*, vol. 3, no. 1, pp. 99–108, 2004.

[11] J.-Y. Le Boudec and M. Vojnović, "Perfect simulation and stationarity of a class of mobility models," in *Proceedings of the 24th Annual Joint Conference of the IEEE Computer and Communications Societies (INFOCOM '05)*, vol. 4, pp. 2743–2754, Miami, Fla, USA, March 2005.

[12] C. Chiang, "Wireless networks multicasting," Ph.D. dissertation, Department of Computer Science, University of California, Los Angeles, Calif, USA, 1998.

[13] B. Liang and Z. J. Haas, "Predictive distance-based mobility management for PCS networks," in *Proceedings of the 18th Annual Joint Conference of the IEEE Computer and Communications Societie (INFOCOM '99)*, vol. 3, pp. 1377–1384, New York, NY, USA, March 1999.

[14] B. Liang and Z. J. Haas, "Predictive distance-based mobility management for multidimensional PCS networks," *IEEE/ACM Transactions on Networking*, vol. 11, no. 5, pp. 718–732, 2003.

[15] C. Bettstetter, "Mobility modeling in wireless networks: categorization, smooth movement, and border effects," *ACM SIGMOBILE Mobile Computing and Communications Review*, vol. 5, no. 3, pp. 55–66, 2001.

[16] X. Hong, M. Gerla, G. Pei, and C. Chiang, "A group mobility model for ad hoc wireless networks," in *Proceedings of the 2nd ACM International Workshop on Modeling, Analysis and Simulation of Wireless and Mobile Systems (MSWiM '99)*, pp. 53–60, Seattle, Wash, USA, August 1999.

[17] F. Bai, N. Sadagopan, and A. Helmy, "The IMPORTANT framework for analyzing the impact of mobility on performance of routing protocols for ad hoc networks," *Ad Hoc Networks*, vol. 1, no. 4, pp. 383–403, 2003.

[18] L. Kleinrock, *Queueing Systems*, vol. 1, John Wiley & Sons, New York, NY, USA, 1975.

[19] C. A. V. Campos, D. C. Otero, and L. F. M. de Moraes, "Realistic individual mobility Markovian models for mobile ad hoc networks," in *Proceedings of IEEE Wireless Communications and Networking Conference (WCNC '04)*, vol. 4, pp. 1980–1985, Atlanta, Ga, USA, March 2004.

[20] Z. J. Haas and M. R. Pearlman, "The performance of query control schemes for the zone routing protocol," *ACM SIGCOMM Computer Communication Review*, vol. 28, no. 4, pp. 167–177, 1998.

[21] P. Johansson, T. Larsson, N. Hedman, B. Mielczarek, and M. Degermark, "Scenario-based performance analysis of routing protocols for mobile ad hoc networks," in *Proceedings of the 5th Annual ACM/IEEE International Conference on Mobile Computing and Networking (MOBICOM '99)*, pp. 195–206, Seattle, Wash, USA, August 1999.

[22] K. Fall and K. Varadhan, *The NS Manual*, The VINT Project, January 2002.

[23] L. Qiming, "The scenario generator: a tool to generate MANET mobility scenarios for NS-2," 2001.

[24] "CRAWDAD Project—A Community Resource for Archiving Wireless Data at Dartmouth," http://crawdad.cs.dartmouth.edu/.